Title

Unidirectional and sustained delivery of the proresolving lipid mediator resolvin D1 from a biodegradable thin film device

Journal

Journal of Biomedical Materials Research Part A, 105(1)

ISSN

1549-3296

Authors

Lance, Kevin D
Chatterjee, Anuran
Wu, Bian
et al.

Publication Date

2017

DOI

10.1002/jbm.a.35861

Peer reviewed

HHS Public Access

Author manuscript

J Biomed Mater Res A. Author manuscript; available in PMC 2018 January 01.

Published in final edited form as:

J Biomed Mater Res A. 2017 January ; 105(1): 31–41. doi:10.1002/jbm.a.35861.

Unidirectional and Sustained Delivery of the Pro-Resolving Lipid Mediator Resolvin D1 from a Biodegradable Thin Film Device

Kevin D. Lance[a,b,**], **Anuran Chatterjee**[c,**], **Bian Wu**[c], **Giorgio Mottola**[c], **Harald Nuhn**[b], **Phin Peng Lee**[a], **Brian E. Sansbury**[d], **Matthew Spite**[d], **Tejal A. Desai**[a,b], and **Michael S. Conte**[c,*]

[a]UC Berkeley - UCSF Graduate Group in Bioengineering. 1700 4th Street, QB3 Byers Hall, Room 203, San Francisco, CA 94158, USA

[b]Department of Bioengineering and Therapeutic Sciences, University of California San Francisco, 1700 4th Street, QB3 Byers Hall, Room 203, San Francisco, California 94158, USA

[c]Cardiovascular Research Institute (CVRI) and Department of Surgery, University of California San Francisco, 555 Mission Bay Blvd. South, room 284-H, San Francisco, California 94143, USA

[d]Center for Experimental Therapeutics and Reperfusion Injury, Department of Anesthesiology, Perioperative and Pain Medicine, Brigham and Women's Hospital and Harvard Medical School, Harvard Institutes of Medicine HIM 830, 77 Avenue Louis Pasteur, Boston, MA 02115, USA

Abstract

Resolvin D1 (RvD1) belongs to a family of endogenously derived pro-resolving lipid mediators that have been shown to attenuate inflammation, activate pro-resolution signaling and promote homeostasis and recovery from tissue injury. In this study we present a poly(lactic-co-glycolic acid) (PLGA) based thin-film device composed of layers of varying ratios of lactic and glycolic acid that elutes RvD1 unidirectionally to target tissues. The device demonstrated sustained release *in vitro* for 56 days with an initial burst of release over 14 days. The asymmetric design of the device released 98% of RvD1 through the layer with the lowest molar ratio of lactic acid to glycolic acid, and the remainder through the opposite side. We validated structural integrity of RvD1 released from the device by mass spectrometry and investigated its bioactivity on human vascular endothelial (EC) and smooth muscle cells (VSMC). RvD1 released from the device attenuated VSMC migration, proliferation and TNF-α induced NF-κB activation, without evidence of cytotoxicity. Delivery of RvD1 to blood vessels was demonstrated *ex vivo* in a flow chamber system using perfused rabbit aortas and *in vivo* in a rat carotid artery model, with the devices applied as an adventitial wrap. Our results demonstrate a novel approach for sustained, local delivery of Resolvin D1 to vascular tissue at therapeutically relevant levels.

Keywords

PLGA; resolvin; inflammation; vascular delivery; wrap

Correspondence to: Dr. Michael S. Conte, 400 Parnassus Avenue, Suite A-581, San Francisco, CA, 94143-0957, USA, michael.conte2@ucsf.edu.

**These authors contributed equally and are co-first authors for this work.

Introduction

Resolvin D1 (7S,8R,17S-trihydroxy-4Z,9E,11E,13Z,15E,19Z-docosahexaenoic acid; RvD1) belongs to a recently discovered class of specialized pro-resolving lipid mediators (SPMs) that promote resolution of inflammation across a wide variety of inflammatory conditions[1] such as inflammatory bowel disease,[2] colitis,[3] sepsis,[4] endotoxin-induced lung[5] and kidney injury,[6] periodontitis[7] and vascular injury.[8,9] SPMs (lipoxins, resolvins, protectins, and maresins) are produced endogenously from dietary omega-6 (arachidonic acid) and omega-3 (docosahexaenoic acid and eicosapentaenoic acid) polyunsaturated fatty acids. These SPMs are locally generated from their precursors via trans-cellular biosynthetic pathways involving lipoxygenases in the inflammatory milieu, and are known to down-regulate pro-inflammatory signaling[10–12] through inhibition of NF-κB activity, attenuation of neutrophil chemotaxis, induction of M1 –M2 macrophage polarization and efferocytosis (clearance of dead cells and leukocytes in the inflammatory zone).

SPMs function as homeostatic autacoids, imparting a resolution phenotype within the local environment that has been demonstrated experimentally across a broad range of inflammatory pathologies.[4,13–16] However, biochemical stability of these free fatty acids and enzymatic inactivation by ubiquitous enzymes such as eicosanoid oxidoreductase[17] may limit spatial effects of SPMs to the immediate tissue environment. In previous animal studies, organically synthesized SPMs were administered through intraperitoneal, subcutaneous, intravenous or intra-arterial methods, which may be inefficient or impractical for clinical use.[3–6,8,9] For example, in the context of vascular injury caused by surgical interventions (e.g. bypass graft or arteriovenous fistula creation), local availability of drugs or biologics may be optimized by a local delivery approach to the surgical field. The therapeutic yield would be further maximized by a delivery system that preferentially delivers its payload towards the target tissue while minimizing losses to surrounding off-target tissues. Sustained, local delivery of SPMs may be highly relevant for vascular pathologies like bypass graft failure where persistent inflammation and subsequent fibrosis are implicated in the pathophysiological response. Other potential applications might include gastrointestinal or urologic procedures, organ transplantation, and microvascular tissue transfers. We sought to develop a biodegradable device for sustained, local and directional delivery of SPM that could be applied in relevant surgical settings, particularly for blood vessel applications.

An optimal drug delivery device for perivascular delivery would release its therapeutic agent at physiologically relevant concentrations selectively to the local vasculature over a sustained period of time (e.g. weeks). Previous attempts at perivascular drug delivery from polymer devices have included particles, wraps, cuffs and hybrid assemblies of PLGA, PCL, or both polymers. These attempts have aimed to regulate inflammation and proliferation with various drugs, such as rapamycin,[18,19] paclitaxel,[18,20,21] cyclosporine A,[22] and sunitinib.[23] However, clinical use of these drugs has been limited due to cytotoxicity, which merits the development of a drug delivery approach focused on SPM (e.g. RvD1). Furthermore, the unique combination of sustained and unidirectional release of a bioactive lipid compound in a flexible thin film (<100μm thickness) device has not previously been demonstrated.

In the present study, we describe a thin polymer device composed of PLGA films of varying ratios of lactic and glycolic acid and loaded with RvD1. Through the use of layers of varying types of PLGA thin films, we aim to achieve directional delivery of RvD1 toward the intended side for drug release, minimizing drug loss to non-target tissues. The thin and pliable nature of such a device facilitates favorable surgical handling, which could allow for therapeutic applications across a broad range of scenarios where sustained, local availability of RvD1 may attenuate tissue damage and restore homeostasis.

Material and Methods

Device Fabrication

PLGA thin films were spun-cast onto polydimethylsiloxane (PDMS, Thermo Fisher Scientific, Waltham, MA) discs from 1 mL solutions of PLGA at 300 mg/mL in 2,2,2-trifluoroethanol (TFE, Sigma-Aldrich, St. Louis, MO). Films were spun-cast at 1000 rpm for 30 seconds, followed by 2000 rpm for 30 seconds. Rectangular (8 × 12 mm) pieces of film were laser cut and assembled into a two- or three-layered device. Drug was loaded onto wraps by pipetting a solution of 100 μg ml^{-1} 17S-Resolvin D1 (RvD1, Cayman Chemical, Ann Arbor, MI) in ethanol onto a piece of PLGA film and allowing the ethanol to evaporate before assembling further layers (Supporting Figure S1). Drug payloads were concentrated in the center of the PLGA film rectangles and away from the outer edges by pipetting the drug in 1 μL increments. In trilayered devices 100 ng was loaded in between both pairs of films for a total of 200 ng RvD1 loaded per device. In bilayered devices used for directional release experiments, 200 ng RvD1 was loaded between the two films. After drug loading, the films were annealed together by an electrified nichrome wire (Consolidated Electronic Wire and Cable, Franklin Park, IL) embedded in a PDMS block. Bilayered devices were made of two identical layers of random copolymers of PLGA with lactic acid:glycolic acid (L:G) ratios of either 50:50 (M_n 38–54 kDa, acid endcap, Sigma-Aldrich), 75:25 (M_n 35–45 kDa, acid endcap, PolySciTech, West Lafayette, IN) or 85:15 (M_n 35–45 kDa, acid endcap, PolySciTech). Trilayered devices were made of 50:50, 75:25 and 85:15 PLGA where the 75:25 PLGA film was placed in between the 50:50 and 85:15 PLGA films. The morphology of thin film devices in cross-section was investigated by scanning electron microscopy (SEM) following freeze-fracturing in liquid nitrogen. Devices to be analyzed were coated with Au/Pd by a Cressington-HR sputter coater and imaged with a Carl Zeiss Ultra 55 field emission scanning electron microscope using a standard Everhart-Thornley secondary electron detector.

In vitro Elution Experiments

Device performance was evaluated *in vitro* with serum-free media (SFM) or PBS as an elution buffer. SFM was composed of DMEM medium was obtained from UCSF Cell Culture Facility and was supplemented with antibiotics and fungicide. Devices were incubated in 300 μL of elution buffer in Eppendorf tubes at 37°C while continuously shaken. At different sampling time-points, elution buffer was completely removed and replaced with fresh buffer. The time-points used for long-term elution studies were 3 hours, 1 day, 4 days, and weeks 1 to 7. Time-points were chosen to resolve RvD1 release soon after immersion (3 hours), within the timeframe of tissue healing (1 day to 1 week), and over the course of

device degradation and payload exhaustion (weeks 2 to 7). Samples were analyzed by 17S-Resolvin D1 enzyme immunoassay (EIA) kits (Cayman Chemical).

Drug Elution Buffer Stability

RvD1 stability in SFM, PBS, and ethanol was evaluated by adding 1 μL of stock RvD1 (100 μg ml^{-1}) via Hamilton syringe to 0.5 mL of each liquid medium in a screw-top tube. Triplicate samples were incubated at 37°C with shaking for 2 days and 7 days, and one set (3 hours) was prepared the same day as analysis by EIA.

Drug Total Payload Release

Maximum recovery of the loaded RvD1 payload was performed by wrap homogenization in a glass dounce homogenizer in ethanol, followed by an *in vitro* elution experiment, as described above, with the elution buffer being pure ethanol. Ethanol was sampled and replaced every day for four days. The ethanol in which the wraps were homogenized was removed and assayed as an initial time-point. This process was also performed using PBS as both the homogenization and elution buffer. Attempts at dissolving devices in organic solvents and recovering RvD1 through solvent evaporation recovered negligible amounts of drug (data not shown).

In vitro Directional Diffusion Chamber Elution Experiments

Directional drug elution was studied by isolating the SFM exposed to each side of a trilayered device in a diffusion chamber. The diffusion chambers were incubated at 37°C with shaking. At different sampling time-points, SFM was completely removed and replaced through the sampling ports of the diffusion chamber using a needle and syringe. Samples were assayed by EIA.

Liquid Chromatography-Tandem Mass Spectrometry

Elution samples of both SFM and PBS from *in vitro* experiments were flash frozen in liquid nitrogen and analyzed by liquid chromatography-tandem mass spectrometry (LC-MS/MS) to evaluate the structural integrity of RvD1 released from the device. One volume of methanol containing internal deuterium-labeled standard (d_5-RvD2) was added to samples to assess extraction recovery. Solid phase extraction and LC-MS/MS analysis were carried out as described previously.[24] Briefly, RvD1 was extracted using C18 solid phase extraction cartridges and an automated extraction system (RapidTrace, Biotage). Following extraction, the methyl formate fractions were placed under a stream of N_2 gas until the solvent evaporated. The samples were then resuspended in methanol:water (50:50) prior to injection. Analysis by LC-MS/MS was conducted using a Poroshell reverse-phase C18 column (100 mm × 4.6 mm × 2.7 μm; Agilent Technologies) on a high performance liquid chromatography system (HPLC; Shimadzu) coupled to a QTrap 5500 mass spectrometer (AB Sciex). The mobile phase consisted of methanol:water:acetic acid (55:45:0.01 vol/vol/vol) and was ramped to 85:15:0.01 (vol/vol/vol) over 10 min, followed by ramping to 98:2:0.01 (vol/vol/vol) over the next 8 min and held for additional 2 min. The entire sample elution was performed using a constant flow rate of 400 μL min^{-1} at a constant temperature of 50°C. The QTrap was operated in negative ionization mode using established scheduled

multiple reaction monitoring (MRM) transitions[25] coupled with information-dependent acquisition (IDA) and enhanced product ion-scanning (EPI). RvD1 was identified using retention time and at least six diagnostic MS/MS ions, as compared with authentic RvD1 standard (Cayman Chemical). LC-MS/MS quantification was not used as the primary means of RvD1 detection due to the large number of samples to be quantified, cost, and logistical efficiencies.

In vitro Bioassay Experiments

Human greater saphenous veins discarded at the time of coronary or peripheral bypass grafting operations at The University of California- San Francisco (approved by the Institutional Review Board; UCSF Committee on Human Research- Number: 10-03395; the committee waived the need for informed consent) were used to prepare primary cell cultures of ECs and VSMCs, as described previously.[26] Cells of passage 3–5 were used for all experiments. Trilayered devices loaded with either RvD1 or ethanol vehicle were placed inside cell media contained in a permeable transwell insert of 0.4um pore diameter (Corning, Tewksbury, MA) and the insert was placed above the cells to deliver RvD1 in the following experiments:

NF-κB Assay (p65 Nuclear Translocation)—VSMCs were grown to 70% confluency in 24-well plates and were exposed to devices placed in transwells for 18 hr followed by addition of TNF-α (10ng ml^{-1}) for 2 hours. Total volume of media used per well was 900ul, with 400ul media placed inside the transwell. At 2 hours post TNF-α addition, transwells were removed, media was saved for RvD1 EIA and cells were fixed with 4% paraformaldehyde then washed with warm PBS. Cells were then treated with 0.5% Triton-X and fixed in ice-cold methanol for 10min. The VSMCs were incubated overnight with anti-p65 antibody in a humidified chamber at 4°C and probed the next day with Alexa-488 secondary antibody and visualized under a fluorescent microscope.

Cell Proliferation Assay—VSMCs (passage 3) were seeded on 6-well plates in 0.5% media and were serum starved for three days. On day four, cells were exposed to 10% media to stimulate proliferation. A control group was exposed to 0.5% media. At the time of exposure to 0.5% and 10% media, a transwell with a vehicle- or RvD1-loaded device was placed in each well. The media was refreshed at days 6 and 8 and total cell counts were calculated on day 10 using a neubauer hemocytometer.

Migration Assays—VSMCs were grown to confluency on 24-well plates and then serum starved overnight in 0.5% media. The following day a scratch was made along the center of the well with a sterile pipette tip and PDGF-BB (platelet-derived growth factor homodimer BB) was added to the wells to stimulate migration, except for control wells. Vehicle- or RvD1-loaded devices in transwells were then placed in each well. The migratory response was quantified by calculating the area of scratch injury at time of injury and 24 hours later using Image J software (NIH). For EC migration assays the same procedure was followed, except cells were grown in gelatin-coated wells and M199 EC-media (Hyclone Inc, Logan, UT) with 10% serum was used to stimulate migration following scratch wounding. In all of these experiments, media was stored for RvD1 EIA.

MTT Assay—VSMCs or ECs were grown to confluence on 24-well plates and were exposed to trilayered PLGA devices as described above in SFM. Cytotoxicity was quantified at 24 hours using a standard MTT Assay kit (Sigma, St Louis, MO).

Ex vivo Flow Chamber for Vascular Delivery

Adventitial drug delivery to blood vessels must overcome transmural pressure and convection forces that tend to resist outside-in diffusion and promote axial removal of liquid phase materials away from the region of interest to the interstitium.[27,28] To study directional drug release from an externally applied device onto the vessel wall, we created an *ex vivo* closed-circuit system with continuous pulsatile flow. Flow-chambers were 3D-printed at the UCSF Center for Advanced Technologies (uPrint SE Plus, Stratasys Inc) and pulsatile flow was provided via an external mechanical pump (Colonial Scientific, Richmond, VA). The circuit was completed by inserting segments of aorta harvested from female New Zealand white rabbits obtained through the UCSF tissue-sharing program. To examine directional delivery, we created a co-axial vessel construct. The inner, target vessel was mounted inside the flow chamber and a trilayered device (85:15 PLGA / 100 ng RvD1 / 75:25 PLGA / 100 ng Rvd1 / 50:50 PLGA) was wrapped around the inner vessel with the 50:50 PLGA side facing inwards towards the vessel. A second, outer vessel was then secured snugly around the device and inner vessel, to model the perivascular soft tissues. All side branches of both the inner and outer vessels were ligated to ensure a closed circuit. The flow chamber was filled with SFM and the mechanical pump was activated to simulate blood flow at approximately 35–40 ml min^{-1}. After 24 hours the inner and outer vessels were removed and homogenized in ice-cold PBS using a glass dounce homogenizer. Lysates were then centrifuged for 15 minutes at 18000 g to remove debris and the supernatant was further purified by centrifuging for 15 minutes at 14000 g through a 30kD cut-off filtration device (Amicon ultra, Millipore, Billerica, MA) prior to RvD1 analysis by EIA.

In vivo Drug Delivery Model

Male Sprague-Dawley rats (400–500 g) were used for *in vivo* experiments under an institutionally approved protocol in which NIH guidelines for the care and use of laboratory animals (NIH Publication #85-23 Rev. 1985) were observed. To evaluate acute drug elution to a vascular arterial target, rats were anesthetized under isoflurane and the left common carotid artery exposed through a midline neck incision. An 8 mm × 12 mm trilayered PLGA device (85:15 PLGA / 100 ng RvD1 / 75:25 PLGA / 100 ng RvD1 / 50:50 PLGA) sterilized by 70% ethanol submersion was wrapped around the common carotid artery, with 50:50 PLGA film facing the artery, and secured with interrupted 7–0 prolene sutures. After 1 hour, the device was removed and both the left and right carotid arteries were harvested and immediately frozen in PBS. Tissue lysates were assayed for RvD1 by EIA as described above.

Statistics

Data are reported as +/− their standard deviation. Statistics were performed using a Student’s t-test with a significance threshold at 0.05.

Results

Device Morphology

Trilayered devices (Figure 1A) were assembled as described above and their morphology was investigated. The PLGA thin films demonstrated the flexibility needed to wrap around vasculature (Figure 1B and 1C). Film thicknesses were as low as 10 μm for individual films, with an average of 50.9 (± 7.6) μm for assembled trilayered devices. 50:50 PLGA films had an average thickness of 12 (± 0.73) μm, 75:25 PLGA films had an average thickness of 9.9 (± 1.1) μm, and 85:15 PLGA films had an average thickness of 26(± 4.0) μm. The PLGA devices were transparent and pliant after fabrication. Analysis of the devices by SEM showed cohesion between the multiple layers of the device without any delamination between layers. In cross-section the devices retained discernible strata corresponding to the original films used to make the device, indicating minimal, if any, mixing of polymers between film layers (Figure 1D).

In vitro RvD1 Release and Stability

We investigated the RvD1 release kinetics of asymmetric trilayered devices designed to preferentially release drug through one side of the device. The devices were designed with a diffusion-blocking layer of 85:15 PLGA, a 75:25 PLGA layer in the middle for slow-release of RvD1, and an inner layer of 50:50 PLGA to allow rapid RvD1 diffusion. Long-term release of RvD1 from trilayered devices showed a biphasic release behavior with more rapid and greater drug release in SFM than in PBS (Figure 2A). After one week of elution, devices in SFM released 4.96 (± 1.89) ng of RvD1 cumulatively, while devices in PBS released 3.67 (± 1.26) ng. The total RvD1 released after three weeks was 16.5 (± 3.41) ng for wraps in SFM, and 8.29 (± 2.96) ng for wraps in PBS. The additional RvD1 released between weeks 3 and 7 was 0.283 ng and 0.345 ng for PBS and SFM, respectively. It is important to note that RvD1 experienced degradation in the elution buffers used (Figure 2B). However, even though RvD1 stability was higher in PBS than SFM, the cumulative RvD1 eluted by a wrap in SFM was nearly twice that of a wrap in PBS. The differences in degradation experienced by devices eluting RvD1 over ten weeks in either SFM or PBS (Figure 2C) combined with the differences in cumulative RvD1 elution suggest that wrap degradation is a factor contributing to increased RvD1 release in SFM.

To evaluate the total loading of RvD1 in the devices, homogenization of devices was performed and either PBS or ethanol as an elution buffer was used for drug elution. The total amount of RvD1 recovered when both homogenizing devices and eluting in ethanol was 168 (± 21.5) ng, or 83.9% of drug loaded (Figure 2D). Using intact devices that had not been homogenized and eluting in ethanol yielded 71.6 (± 19.7) ng or 35.8% of drug loaded. Using homogenized devices but using PBS as the elution buffer drops the amount of recovered RvD1 to 27.8 (± 3.41) ng, or 13.9% of drug loaded (Figure 2E). The difference in recovered RvD1 between homogenized and intact devices eluting in ethanol further demonstrates that surface area, which was increased by degradation in other elution experiments, is a factor in RvD1 elution.

Directional Chamber *in vitro* RvD1 Release

Directional release from trilayered devices was investigated by observing the release behavior of RvD1 from the *in vitro* elution behavior of bilayered devices, and from the behavior of trilayered devices in diffusion chambers. To study RvD1 release from trilayered devices, a two-sided diffusion chamber was used to isolate the SFM exposed to each side of the devices (Figure 3A and 3B). Directional release from the trilayered devices showed a statistically significant ($p < 0.05$) difference between the two sides as early as day 1 (Figure 3C). At day 14, 97.9% of the total cumulative amount of RvD1 released on both sides of the device had been released from the 50:50 PLGA side.

In vitro RvD1 Release from Bilayered Devices

Bilayered PLGA devices composed of two identical pieces of PLGA were used to isolate and investigate the release properties of PLGA thin films with different L:G ratios in *in vitro* release experiments in Eppendorf tubes (Figure 3D). Bilayered devices of 50:50 L:G ratio showed the fastest release, with 51% of cumulative total released by day 3 and a total cumulative release of 25 (± 3.3) ng. Increasing the L:G ratio to 75:25 resulted in a slower release rate, with 46% released by day 7, and 11 (± 4.6) ng cumulatively released by day 14. Drug release from 85:15 PLGA devices was above the lower limit of detection (8 pg mL^{-1}) at days 7, 12, and 14, but the total cumulative RvD1 release did not exceed 0.2 ng. The relatively inhibited diffusion of drug through 85:15 PLGA layers supports its use as a blocking layer for RvD1 diffusion. Of note, the release of RvD1 from the 85:15/85:15 bilayered device demonstrates the amount of RvD1 that is released through the edges and through the 85:15 film itself. Since RvD1 release from the edges may be at most 0.2 ng of cumulative drug release, then the release of RvD1 through device edges can only contribute a negligible amount to total device release behavior that is on the order of tens of nanograms.

Assessment of RvD1 Release and Stability by LC-MS/MS

We assessed the structural integrity of RvD1 loaded and released from the trilayered device by LC-MS/MS. Using multiple reaction monitoring (MRM), authentic RvD1 standard showed a retention time of 11.7 minutes (Figure 4A) and a distinct peak at this same retention time was observed for both sealed (heated by nichrome wire, see methods) and unsealed devices in PBS at a 3 hour time-point (Figure 4B–C). Samples of device elution experiments using SFM as an elution buffer showed the characteristic RvD1 peak in addition to additional non-RvD1 peaks (Figure 4D). Full MS/MS spectra of RvD1 released from the device showed diagnostic fragmentation ions consistent with that observed for authentic RvD1 (Figure 4E).

In vitro Biological Assays with RvD1 Eluting Trilayered Devices

The *in vitro* cell-based assays tested the bioactivity of RvD1 released from trilayered devices. RvD1 has been shown previously to inhibit VSMC migration, proliferation, NF-κB activity, and to attenuate inflammatory responses in both smooth muscle and endothelial cells.[9] Bioassays testing these vascular cell responses were chosen to confirm bioactivity of RvD1 released from the thin film devices. RvD1-loaded devices inhibited NF-κB activity in

VSMC with a 36% reduction of nuclear p65 translocation after TNF-α stimulus, as compared to vehicle-loaded devices (Figure 5A, Supporting Figure S2). RvD1-loaded devices also produced a robust inhibition in VSMC proliferation by as much as 39% when compared to vehicle-loaded devices (Figure 5B). Similarly, RvD1-loaded devices attenuated VSMC migration by 22% when compared to vehicle-loaded devices (Figure 5C). We also investigated the response of endothelial cells to RvD1-loaded devices in the scratch injury model and found that exposure of endothelial cells to these devices produced no discernible alterations in the endothelial wound healing response (Supporting Figure S3), suggesting that endothelial migratory function is retained. Moreover, neither RvD1 nor vehicle-loaded devices showed evidence of vascular cell or endothelial cytotoxicity (Supporting Figure S4). In all our *in vitro* bioassays, the recovered media at the termination of the experiment showed RvD1 levels in the low nanomolar range (5–50 nM).

Ex vivo and *in vivo* Delivery of RvD1

A method for extracting RvD1 from rabbit aortic tissue was validated by analyzing aortic segments spiked with an RvD1 standard (Supporting Figure S5). We used this method to investigate short-term unidirectional RvD1 release from devices in *ex vivo* tissue in a closed-loop system with pulsatile flow (Figure 6A, Supporting Figure S6). A segment of rabbit aorta was mounted in the flow system, a device was placed circumferentially around it, and then a second aortic segment was tightly wrapped external to the device. RvD1 levels measured in the outer vessel after 24 hours were found to be 0.094 (± 0.023) pg RvD1 per mg artery, versus 0.41 (± 0.17) pg RvD1 per mg artery in the inner vessel (Figure 6B, $p = 0.03$). When not normalized to arterial mass, the total mass of RvD1 detected in the inner layer (36.8 ± 15.4 pg) was still significantly greater than the mass in the outer layer (15.2 ± 15.4 pg, $p<0.01$). These data demonstrate successful delivery of RvD1 into the underlying vessel under conditions of flow, with a marked asymmetry favoring elution from the 50:50 PLGA side.

Finally, we tested *in vivo* RvD1 release in an acute rodent model of drug delivery to carotid arteries. We found that application of the trilayered device around the left carotid artery (LCA, Figure 6C) resulted in significantly higher levels of immunoreactive RvD1 in the arterial tissue compared to contralateral untreated controls (native right carotid artery, RCA) at one hour post-application (Figure 6D). The level of RvD1 in LCA was 0.63 (± 0.060) pg RvD1 per mg tissue compared to 0.12 (± 0.10) pg RvD1 per mg tissue in RCA.

Discussion

PLGA is well documented as a biodegradable polymer with a long history in the field of controlled drug delivery. The described PLGA thin film device allows for local and sustained drug (RvD1) release, which is particularly relevant for surgical applications where target tissues such as vascular anastomoses are accessible, and persistent inflammation an important source of aberrant healing and complications. SPMs, such as RvD1, have been demonstrated to carry therapeutic potential in the context of surgical injury.[8,9] However, local delivery of bioactive lipid mediators has remained relatively unexplored.

Rodent studies using RvD1 and other SPMs in inflammatory pathologies have largely been limited to systemic intravenous, subcutaneous, intraperitoneal and intraarterial delivery.[3–9] In one recent study, RvD1 was incorporated into chitosan scaffolds by adsorption followed by lyophilization,[29] and was used locally to favorably modulate the immune response in a mouse model of air-pouch induced inflammation. Similarly, humanized leukocyte-derived nanoparticles incorporating RvD1 or lipoxin A_4, another SPM analog, has been demonstrated to be effective in the context of murine models of inflammation.[30] However, neither of these studies demonstrates sustained release. Furthermore, these delivery systems also lack the ability to direct their payload preferentially towards target tissues. Here we demonstrate a perivascular wrap device that incorporates thin film layers of various compositions of PLGA to release RvD1 in a unidirectional manner over a period of several weeks. Our device is thin and compliant, allowing for potential utility in a variety of surgical settings, including coronary and peripheral bypass, hemodialysis access fistulas, organ transplantation, microvascular tissue transfers and gastrointestinal or urologic anastomoses. Furthermore, this design is relevant for other similar bioactive lipid or lipophilic molecules, such as other SPMs or prostanoids, which have a broad range of effects on inflammation, thrombosis, fibrosis, and pain.

The described device delivers RvD1 in a sustained manner, demonstrating release of the drug over the first three weeks in an initial burst, followed by detectable levels of RvD1 (>8 pg mL^{-1}) for the remaining weeks of elution. The dependence of the device elution behavior on the elution buffer is informative towards the mechanism of drug release. The increased levels of RvD1 release in the presence of SFM, and the increased degradation of the devices in SFM as compared to PBS, together suggests that degradation of the device films is an important factor in RvD1 release. At the same time, it must be noted that degradation of RvD1 in various media is a confounding factor in the analysis of the elution behavior of the device and the achievement of mass balance between drug loading and release. The identification of an elution buffer that preserves RvD1 stability, and the development of second-generation SPMs with improved stability,[31] will enable more complete characterization of the elution behavior of this type of PLGA thin film device.

The incorporation of RvD1 into our device without exposure to polymerizing radicals or reactive solvents allows us to minimize the impact of the loading process on the stability and bioactivity of the drug. However, the use of PBS and SFM as elution buffers presents difficulties, as these buffers reduce the stability of RvD1, but also influence the device degradation, which plays a key role in drug release. Meanwhile, ethanol as an elution buffer preserves stability but does not drive device degradation. *In vitro* confirmation of RvD1 activity in cellular assays validated the elution of bioactive RvD1 from the devices, while EIA detection used for *in vivo* experiments further verified the increased presence of RvD1 in blood vessels following device implantation. LC-MS/MS analysis of elution buffers collected from trilayered wrap elution experiments revealed the presence of RvD1 that matched the retention time of authentic RvD1 in addition to the presence of degradation side products. However, LC-MS/MS analysis of RvD1 eluted in PBS from both sealed and unsealed devices retains stability, showing that the fabrication of trilayered devices does not degrade its RvD1 payload and the device is able to elute intact drug. Furthermore, in our

RvD1 release studies with carotid artery models, EIA analysis has confirmed the delivery of RvD1 from our devices into the target tissue.

The trilayered devices demonstrated directionality of RvD1 release, as faster release of RvD1 occurs from the 50:50 PLGA side while minimal release is observed from the 85:15 PLGA side. In diffusion chambers studies, the 50:50 PLGA side readily eluted RvD1 while the 85:15 PLGA side effectively blocked all release. Further analysis of the diffusion of RvD1 using bilayered devices demonstrated results consistent with the diffusion chambers studies. Bilayered PLGA devices composed of films of varying L:G ratios showed slower drug release as the percentage of lactic acid monomer was increased. While different total amounts of RvD1 were released from devices of different copolymers, attributable to differences in hydrophobicity and degradation rate, the relative release rates of the devices were the factor used in verifying the properties of RvD1 diffusing through each PLGA copolymer. The elution behavior of the copolymers in isolation ultimately gives support to the directional properties of the trilayered device design. Additionally, *ex vivo* models of unidirectional diffusion in vascular tissues also show a preference for inward RvD1 release even when opposing the pressure gradients of a pulsatile flow system.

RvD1 has been shown to impart protection in the context of arterial injury (restenosis),[8,9] inflammatory bowel disease,[3] ischemia/reperfusion,[6] and endotoxin induced acute kidney injury.[32] Vascular inflammatory diseases, like atherosclerosis and restenosis, are associated with endothelial injury and vascular smooth muscle cell proliferation and migration within the vessel wall that results in intimal hyperplasia. We demonstrate here that RvD1 released from the devices *in vitro* promotes an anti-inflammatory phenotype in vascular smooth muscle cells by attenuating their proliferation, migration and NF-κB activation. We believe this device has therapeutic potential in a variety of surgical settings such as bypass grafting, and recent work using these devices has demonstrated reduced inflammation and neointimal hyperplasia in a rat model of carotid angioplasty.[33] Future work will continue to refine and develop the thin film SPM-eluting device for preclinical studies, and explore new surgical applications.

Conclusions

We have developed a flexible, surgically adaptable, perivascular thin film PLGA device capable of sustained and unidirectional release of the pro-resolving lipid mediator RvD1 to the vasculature. Eluted RvD1 was identified by immunologic detection in an enzyme immunoassay and by LC-MS/MS analysis, and exhibited biological activity on human vascular smooth muscle cells without associated cytotoxicity. These devices were able to deliver therapeutically relevant levels of RvD1 to vascular tissues both *ex vivo* and *in vivo*. Furthermore, the pliable nature of the device allows for direct adherence to blood vessels, and is thus applicable to a variety of acute and sub-acute inflammatory pathologies, such as ischemia-reperfusion, endotoxin-induced injury and vascular injury. This biodegradable device holds therapeutic potential for a broad range of surgical interventions where sustained local delivery of pro-resolving lipid mediators may impart beneficial effects.

Supplementary Material

Refer to Web version on PubMed Central for supplementary material.

Acknowledgments

The authors declare no conflict of interest. The work was supported by funds from National Institutes of Health (HL106173, GM095467, M.S.; RO1 HL119508, M.S.C.; HL123318-01A1, B.W.), Vascular Intervention/Innovation and Therapeutic Advances contract (HHSN268201400005C). Dr Chatterjee is partly funded by American Heart Association- Scientist Development Grant (13SDG16940069). We gratefully acknowledge use of the Carl Zeiss Ultra 55 FE-SEM and supporting equipment at SF State. The FE-SEM and supporting facilities were obtained under NSF-MRI award #0821619 and NSF-EAR award #0949176, respectively.

References

1. Serhan CN. Pro-resolving lipid mediators are leads for resolution physiology. Nature. 2014; 510:92–101. [PubMed: 24899309]
2. Weylandt KH, Kang JX, Wiedenmann B, Baumgart DC. Lipoxins and resolvins in inflammatory bowel disease. Inflamm Bowel Dis. 2007; 13:797–799. [PubMed: 17262807]
3. Bento AF, Claudino RF, Dutra RC, Marcon R, Calixto JB. Omega-3 fatty acid-derived mediators 17(R)-hydroxy docosahexaenoic acid, aspirin-triggered resolvin D1 and resolvin D2 prevent experimental colitis in mice. J Immunol. 2011; 187:1957–1969. [PubMed: 21724996]
4. Spite M, Norling LV, Summers L, Yang R, Cooper D, Petasis Na, Flower RJ, Perretti M, Serhan CN. Resolvin D2 is a potent regulator of leukocytes and controls microbial sepsis. Nature. 2009; 461:1287–1291. [PubMed: 19865173]
5. Wang B, Gong X, Wan JY, Zhang L, Zhang Z, Li HZ, Min S. Resolvin D1 protects mice from LPS-induced acute lung injury. Pulm Pharmacol Ther. 2011; 24:434–441. [PubMed: 21501693]
6. Duffield JS, Hong S, Vaidya VS, Lu Y, Fredman G, Serhan CN, Bonventre JV. Resolvin D series and protectin D1 mitigate acute kidney injury. J Immunol. 2006; 177:5902–5911. [PubMed: 17056514]
7. Fredman G, Oh SF, Ayilavarapu S, Hasturk H, Serhan CN, van Dyke TE. Impaired phagocytosis in localized aggressive periodontitis: Rescue by resolvin E1. PLoS One. 2011; :6.doi: 10.1371/journal.pone.0024422
8. Akagi D, Chen M, Toy R, Chatterjee a, Conte MS. Systemic delivery of proresolving lipid mediators resolvin D2 and maresin 1 attenuates intimal hyperplasia in mice. FASEB J. 2015; 29:2504–2513. [PubMed: 25777995]
9. Miyahara T, Runge S, Chatterjee A, Chen M, Mottola G, Fitzgerald JM, Serhan CN, Conte MS. D-series resolvin attenuates vascular smooth muscle cell activation and neointimal hyperplasia following vascular injury. FASEB J. 2013; 27:2220–2232. [PubMed: 23407709]
10. Fredman G, Serhan CN. Specialized proresolving mediator targets for RvE1 and RvD1 in peripheral blood and mechanisms of resolution. Biochem J. 2011; 437:185–197. [PubMed: 21711247]
11. Serhan CN, Chiang N. Resolution phase lipid mediators of inflammation: Agonists of resolution. Curr Opin Pharmacol. 2013; 13:632–640. [PubMed: 23747022]
12. Lee CH. Resolvins as new fascinating drug candidates for inflammatory diseases. Arch Pharm Res. 2012; 35:3–7. [PubMed: 22297737]
13. Campbell EL, Louis Na, Tomassetti SE, Canny GO, Arita M, Serhan CN, Colgan SP. Resolvin E1 promotes mucosal surface clearance of neutrophils: a new paradigm for inflammatory resolution. FASEB J. 2007; 21:3162–3170. [PubMed: 17496159]
14. Chiang N, Fredman G, Bäckhed F, Oh SF, Vickery T, Schmidt Ba, Serhan CN. Infection regulates pro-resolving mediators that lower antibiotic requirements. Nature. 2012; 484:524–528. [PubMed: 22538616]
15. Fullerton JN, O'Brien AJ, Gilroy DW. Lipid mediators in immune dysfunction after severe inflammation. Trends Immunol. 2014; 35:12–21. [PubMed: 24268519]

16. Kasuga K, Yang R, Porter TF, Agrawal N, Petasis Na, Irimia D, Toner M, Serhan CN. Rapid appearance of resolvin precursors in inflammatory exudates: novel mechanisms in resolution. J Immunol. 2008; 181:8677–8687. [PubMed: 19050288]
17. Sun YP, Oh SF, Uddin J, Yang R, Gotlinger K, Campbell E, Colgan SP, Petasis NA, Serhan CN. Resolvin D1 and its aspirin-triggered 17R epimer: Stereochemical assignments, anti-inflammatory properties, and enzymatic inactivation. J Biol Chem. 2007; 282:9323–9334. [PubMed: 17244615]
18. Pires NMM, van der Hoeven BL, de Vries MR, Havekes LM, van Vlijmen BJ, Hennink WE, Quax PHa, Jukema JW. Local perivascular delivery of anti-restenotic agents from a drug-eluting poly(epsilon-caprolactone) stent cuff. Biomaterials. 2005; 26:5386–94. [PubMed: 15814137]
19. Yu X, Takayama T, Goel Sa, Shi X, Zhou Y, Kent KC, Murphy WL, Guo LW. A rapamycin-releasing perivascular polymeric sheath produces highly effective inhibition of intimal hyperplasia. J Control Release. 2014; 191:47–53. [PubMed: 24852098]
20. Kohler TR, Toleikis PM, Gravett DM, Avelar RL. Inhibition of neointimal hyperplasia in a sheep model of dialysis access failure with the bioabsorbable Vascular Wrap paclitaxel-eluting mesh. J Vasc Surg. 2007; 45:1029–1037. [PubMed: 17466798]
21. Signore PE, Machan LS, Jackson JK, Burt H, Bromley P, Wilson JE, McManus BM. Complete inhibition of intimal hyperplasia by perivascular delivery of paclitaxel in balloon-injured rat carotid arteries. J Vasc Interv Radiol. 2001; 12:79–88. [PubMed: 11200358]
22. Kanjickal D, Lopina S, Evancho-Chapman MM, Schmidt S, Donovan D. Sustained local drug delivery from a novel polymeric ring to inhibit intimal hyperplasia. J Biomed Mater Res A. 2010; 93:656–65. [PubMed: 19610053]
23. Sanders WG, Hogrebe PC, Grainger DW, Cheung AK, Terry CM. A biodegradable perivascular wrap for controlled, local and directed drug delivery. J Control Release. 2012; 161:81–9. [PubMed: 22561340]
24. Colas RA, Shinohara M, Dalli J, Chiang N, Serhan CN. Identification and signature profiles for pro-resolving and inflammatory lipid mediators in human tissue. Am J Physiol Cell Physiol. 2014; 307:C39–C54. [PubMed: 24696140]
25. Dalli J, Serhan CN. Specific lipid mediator signatures of human phagocytes: Microparticles stimulate macrophage efferocytosis and pro-resolving mediators. Blood. 2012; 120:60–73.
26. Chatterjee A, Sharma A, Chen M, Toy R, Mottola G, Conte MS. The Pro-Resolving Lipid Mediator Maresin 1 (MaR1) Attenuates Inflammatory Signaling Pathways in Vascular Smooth Muscle and Endothelial Cells. PLoS One. 2014; 9:e113480. [PubMed: 25409514]
27. Hwang CW, Edelman ER. Arterial ultrastructure influences transport of locally delivered drugs. Circ Res. 2002; 90:826–832. [PubMed: 11964377]
28. Lovich MA, Philbrook M, Sawyer S, Weselcouch E, Edelman ER. Arterial heparin deposition: role of diffusion, convection, and extravascular space. Am J Physiol. 1998; 275:H2236–H2242. [PubMed: 9843824]
29. Vasconcelos DP, Costa M, Amaral IF, Barbosa Ma, Águas AP, Barbosa JN. Development of an immunomodulatory biomaterial: Using resolvin D1 to modulate inflammation. Biomaterials. 2015; 53:566–573. [PubMed: 25890752]
30. Norling LV, Spite M, Yang R, Flower RJ, Perretti M, Serhan CN. Cutting edge: Humanized nano-proresolving medicines mimic inflammation-resolution and enhance wound healing. J Immunol. 2011; 186:5543–5547. [PubMed: 21460209]
31. Orr SK, Colas Ra, Dalli J, Chiang N, Serhan CN. Proresolving actions of a new resolvin D1 analog mimetic qualifies as an immunoresolvent. Am J Physiol - Lung Cell Mol Physiol. 2015; 308:L904–L911. [PubMed: 25770181]
32. Chen J, Shetty S, Zhang P, Gao R, Hu Y, Wang S, Li Z, Fu J. Aspirin-triggered resolvin D1 down-regulates inflammatory responses and protects against endotoxin-induced acute kidney injury. Toxicol Appl Pharmacol. 2014; 277:118–123. [PubMed: 24709673]
33. Wu B, Mottola G, Chatterjee A, Lance KD, Chen M, Siguenza IO, Desai TACM. Perivascular delivery of Resolvin D1 inhibits neointimal hyperplasia in a rat model of arterial injury. J Vasc Surg. 2016; doi: 10.1016/j.jvs.2016.01.030

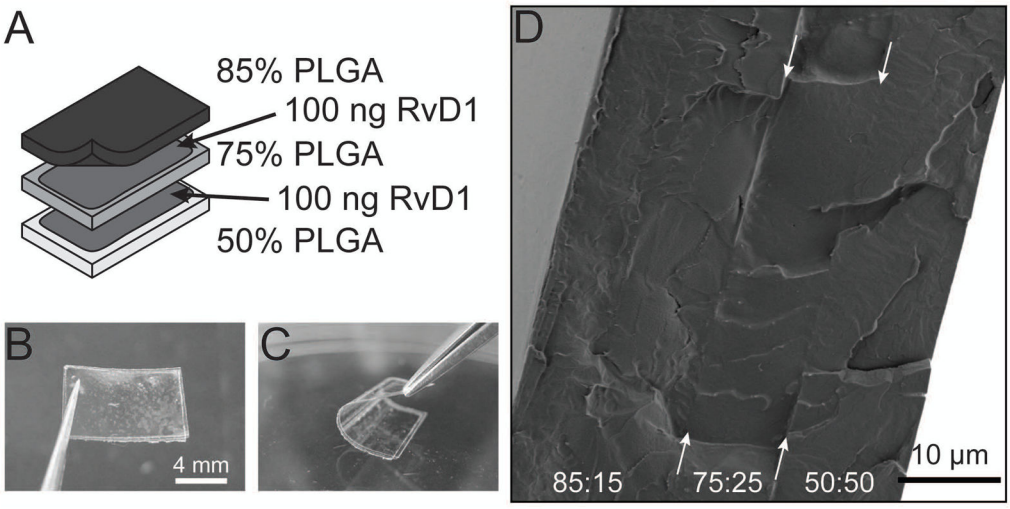

Figure 1.

Assembly and morphology of PLGA devices. (A) Schematic diagram of the assembly of trilayered devices. (B–C): Picture of the trilayered device in flat (B) and bent (C) form showing film flexibility. (D) Scanning electron micrograph of cross-section of a trilayered device with PLGA ratios of each layer labelled. Arrows indicate film interfaces.

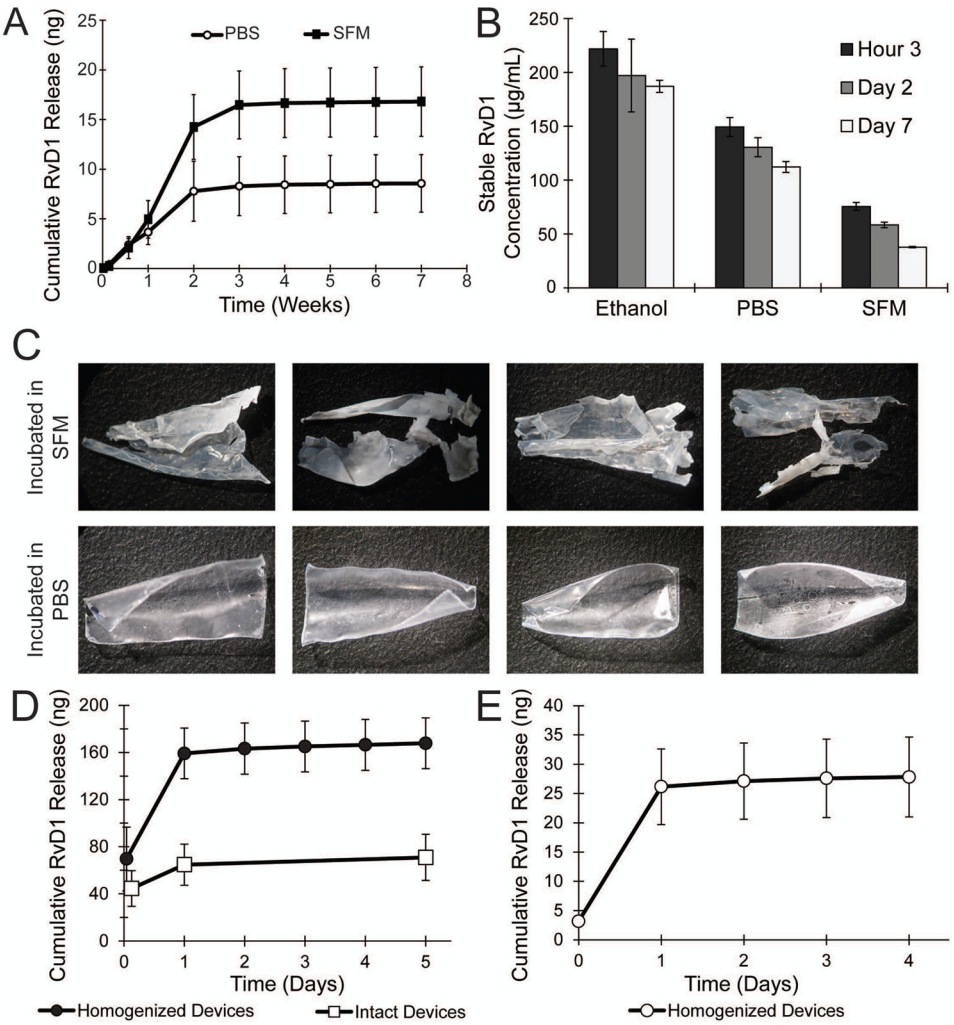

Figure 2.

Elution characteristics of trilayered PLGA devices. (A) Cumulative RvD1 release from trilayered PLGA devices in PBS and SFM elution buffers (n=5 for each buffer). (B) Stability of RvD1 by EIA in ethanol, PBS, and SFM (n=3 for each time-point). (C) Images of devices following 10 weeks of exposure to SFM (top row) or PBS (bottom row). (D) Cumulative RvD1 release in ethanol either with or without device homogenization (n=3 for each condition). (E) Cumulative RvD1 release in PBS after device homogenization (n=3). Error bars are standard deviations and * : $p \leq 0.05$ by Student's t-test.

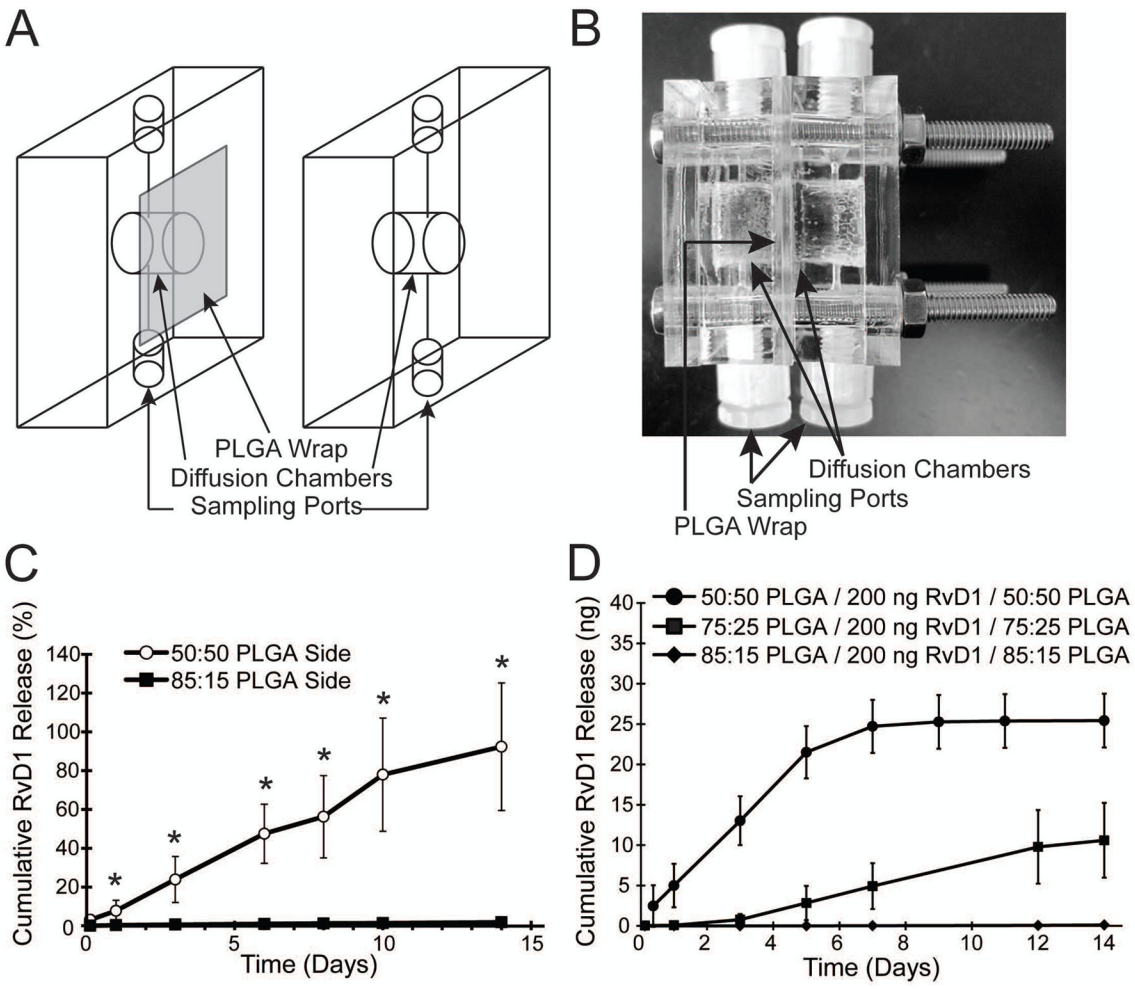

Figure 3.

Directional release of RvD1 from trilayered devices and non-directional bilayered device release. (A) Schematic representation of the device (B) used to study RvD1 release from two sides of the devices. RvD1-loaded devices were placed in between the two halves of the cube, and diffusion chambers were filled with media, which was sampled and replaced through the side ports at each time-point. (C) Cumulative RvD1 released from each side of the trilayered PLGA construct. * = $p<0.05$ between sides by Student's t-test. (n=4). (D) RvD1 release from bilayered devices of two identical PLGA films with elution performed in Eppendorf tubes (n=3 for each condition).

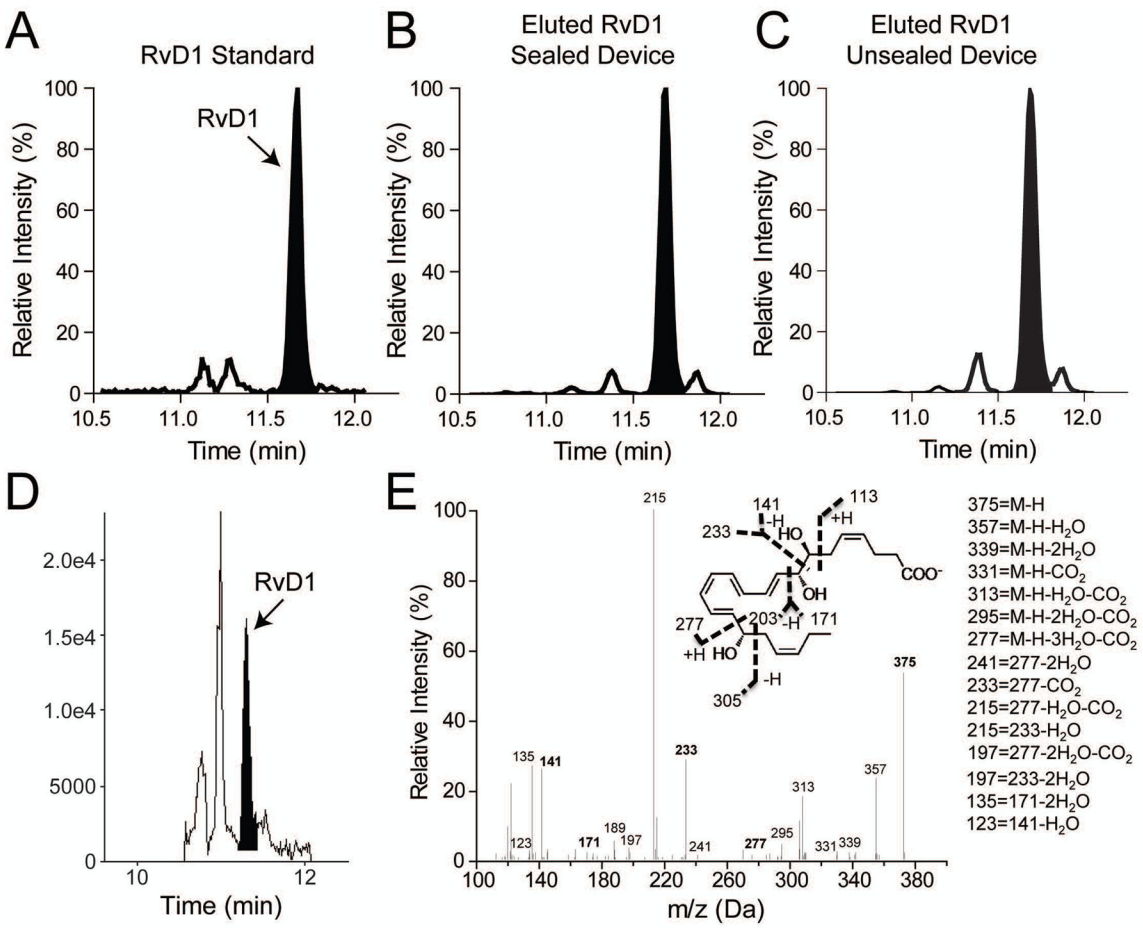

Figure 4.

Identification and quantification of RvD1 released from trilayered PLGA devices. Representative MRM chromatograms are of (A) RvD1 standard, (B) RvD1 released in PBS from a sealed trilayered device, and (C) RvD1 released in PBS from an unsealed device. (D) RvD1 released in SFM from a sealed device. RvD1 released was identified using multiple reaction monitoring (MRM), retention time and diagnostic MS/MS fragmentation ions as compared with authentic RvD1 standard. The retention time matching the RvD1 standard (11.7 min) is shaded in black. (E) Full MS/MS spectra of eluted RvD1 with diagnostic fragmentation ions used for identification indicated as inset.

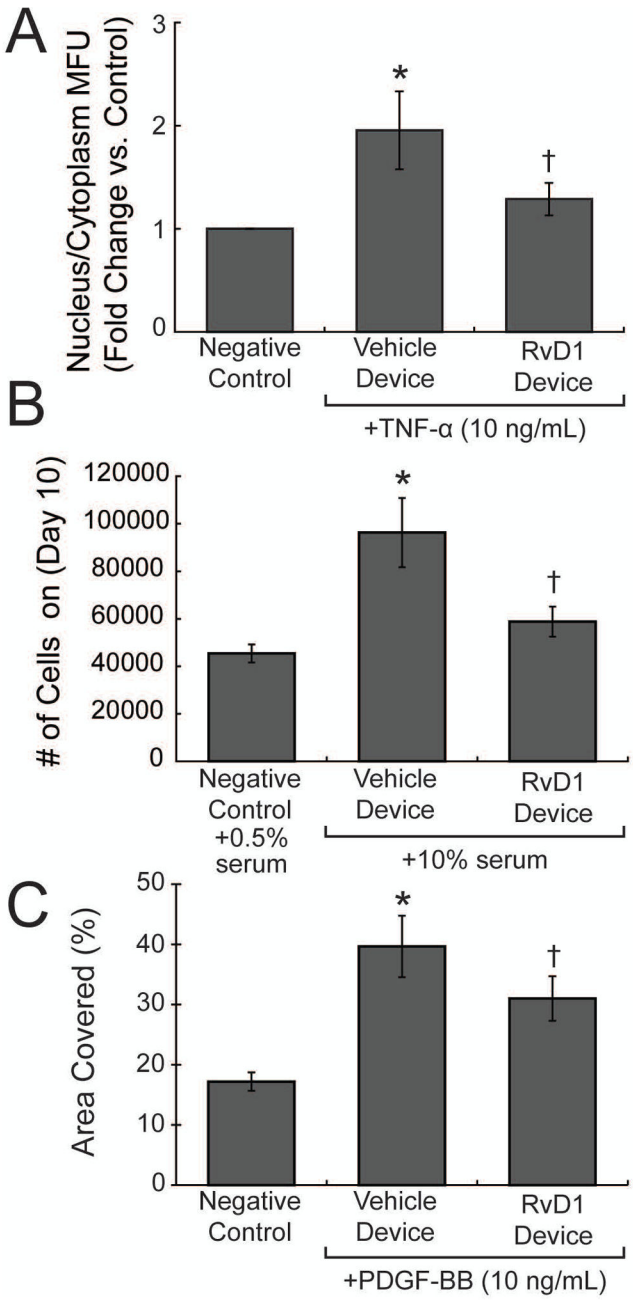

Figure 5.

Biological activity of RvD1 released from trilayered devices. (A) Human vascular smooth muscle cells were incubated with vehicle- or RvD1-loaded device in a transwell for 18hr, followed by vehicle or TNF-α (10ng ml^{-1}) for 2 hours, in the presence of the device. N=3 per group and multiple images were taken from each well at random to quantify net p65 nuclear translocation. (B) VSMC were seeded in 6 well plates and after 2 days of serum starvation, were exposed to 10% serum containing media (day 0) as a proliferative signal in the presence of vehicle- or RvD1-loaded devices. Cells were counted at day 10. N=3 per group. (C) VSMC was grown to confluency in 24-well plates and the area of migration was

quantified at 24 hours following a scratch wound in the presence of PDGF-BB (10 ng ml^{-1}). RvD1-loaded devices inhibited VSMC migration significantly compared to vehicle-wraps. N=4 per group. * = $p<0.05$ from vehicle device controls; † = $p<0.05$ from vehicle device exposed to TNF-α, 10% media, or PDGF-BB, by Student's t-test.

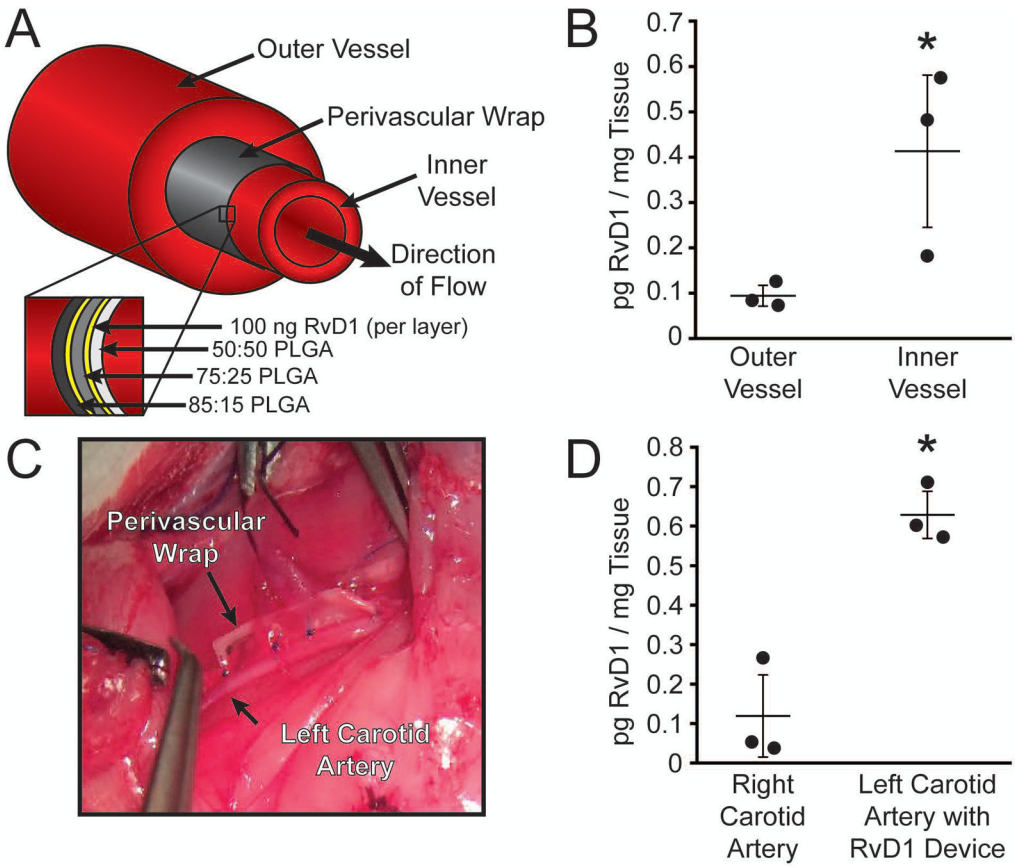

Figure 6.

Unidirectional release of RvD1 from trilayered devices. (A) Schematic diagram of an *ex vivo* closed-circuit flow system. An inner vessel was secured and sealed to a flow chamber with SFM used to generate pulsatile flow at physiologic flow rates supplied by an external pump. The trilayered wrap was then secured to the vessel with the 50:50 PLGA side facing inwards. A second vessel was secured around the wrap and VSMC media was placed in the chamber surrounding the vessels and the system was allowed to run for 24 hours. (C) *In vivo* images of a trilayered device secured around the left carotid artery. (B, D) Net RvD1 uptake by the *ex vivo* vessels and carotid arteries as measured by EIA (n=3). *: $p \leq 0.05$ compared to blank wrap controls by Student's t-test.